Plasma turbulence in the interstellar medium

Katia FERRIÈRE

Institut de Recherche en Astrophysique et Planétologie,
Observatoire Midi-Pyrénées, Toulouse, France

Virtual Nordic Dynamo Seminar

May 26, 2020

Outline

Outline

1. Introduction
2. Effects of radio wave propagation
   - Dispersion of pulsar signals
   - Interstellar scattering
   - Faraday rotation
3. Radio polarized emission
   - Synchrotron emission
   - Faraday tomography

Observational evidence

Map of HI 21 cm emission $(\Delta\alpha \times \Delta\delta = 205^\circ \times 40^\circ)$

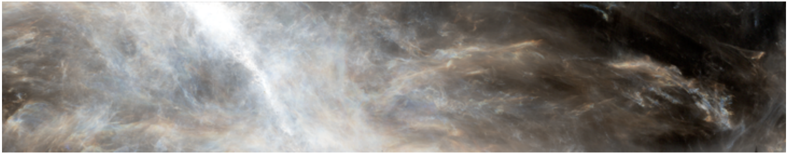

GALFA HI Survey (2015)

Phases of the interstellar medium

	molecular	cold atomic	warm atomic	warm ionized	hot ionized
T [K]	$10 - 20$	$50 - 100$	$10^3 - 10^4$	$\sim 10^4$	$\sim 10^6$
$n_{\rm H}$ [cm^{-3}]	$10^2 - 10^6$	$20 - 50$	$0.2 - 2$	$0.1 - 0.5$	$0.003 - 0.01$
$\frac{n_{\rm e}}{n_{\rm H}}$	$\lll 1$	$(0.3 - 1)\,10^{-3}$	$0.01 - 0.05$	≈ 1	≈ 1.2
B [μG]	> 5	≈ 5	≈ 5	≈ 5	≈ 5

Phases of the interstellar medium

	molecular	cold atomic	warm atomic	warm ionized	hot ionized
T [K]	$10 - 20$	$50 - 100$	$10^3 - 10^4$	$\sim 10^4$	$\sim 10^6$
n_{H} [cm^{-3}]	$10^2 - 10^6$	$20 - 50$	$0.2 - 2$	$0.1 - 0.5$	$0.003 - 0.01$
$\frac{n_e}{n_{\mathrm{H}}}$	$\lll 1$	$(0.3 - 1)\,10^{-3}$	$0.01 - 0.05$	≈ 1	≈ 1.2
B [μG]	> 5	≈ 5	≈ 5	≈ 5	≈ 5

$P_{\mathrm{th}} \sim P_{\mathrm{m}}$ or $\beta \equiv \frac{P_{\mathrm{th}}}{P_{\mathrm{m}}} \sim 1$

☞ Thermal-magnetic equipartition

Phases of the interstellar medium

	molecular	cold atomic	warm atomic	warm ionized	hot ionized
T [K]	$10 - 20$	$50 - 100$	$10^3 - 10^4$	$\sim 10^4$	$\sim 10^6$
$n_{\rm H}$ [cm^{-3}]	$10^2 - 10^6$	$20 - 50$	$0.2 - 2$	$0.1 - 0.5$	$0.003 - 0.01$
$\frac{n_{\rm e}}{n_{\rm H}}$	$\lll 1$	$(0.3 - 1)\ 10^{-3}$	$0.01 - 0.05$	≈ 1	≈ 1.2
B [μG]	> 5	≈ 5	≈ 5	≈ 5	≈ 5

L [pc]		10	30	30	100
V [km s^{-1}]		3	10	10	30
Re		4×10^{10}	10^7	5×10^7	10^2
$\mathrm{Re_m}$		7×10^{14}	3×10^{18}	5×10^{18}	5×10^{22}

Interstellar turbulence

- $\mathrm{Re} \equiv \frac{V\,L}{\nu} \gg 1$ & $\mathrm{Re_m} \equiv \frac{V\,L}{\eta} \gg 1$

  ☞ Fully developed turbulence & magnetic field amplification

- $\mathcal{M}_\mathrm{s} \equiv \frac{V}{C_\mathrm{s}} \sim 1$ & $\mathcal{M}_\mathrm{A} \equiv \frac{V}{V_\mathrm{A}} \sim 1$

  ☞ Turbulence is trans-sonic & trans-Alfvénic

- $\beta \sim 1$ & $\mathcal{M}_\mathrm{s} \sim 1$ & $\mathcal{M}_\mathrm{A} \sim 1$

  ☞ Thermal-magnetic-turbulent equipartition

Turbulence $\Rightarrow$ energy cascade

Sources of turbulence

- Stellar feedback
  - Supernova explosions
  - Stellar winds
  - Protostellar outflows
  - Stellar ionizing radiation
- Galactic rotation
  - Shocks at spiral arms
  - Shear instablility
  - Magneto-rotational instablility

Energy cascade

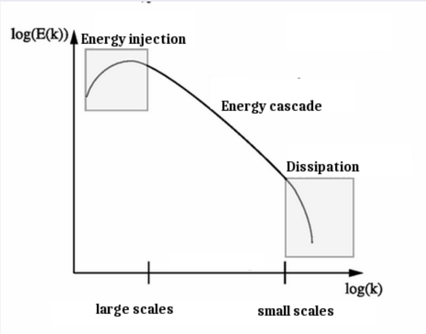

Observational diagnostics

- High-resolution spectroscopy

  ☞ $\delta\vec{v}$

- High-resolution imaging (CO, HI, Hα, dust ...)

  ☞ δn

- Polarization observations (synchrotron, dust, stars ...)

  ☞ $\delta\vec{B}$

- Effects of radio wave propagation

  ☞ $\delta n_{\rm e}$, δB in warm ionized medium [WIM]

Observational diagnostics

- High-resolution spectroscopy

☞ $\delta\vec{v}$

PPP space

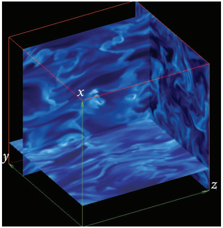

Alejandro Esquivel, MFUVI (2017)

$\Longrightarrow$

PPV space

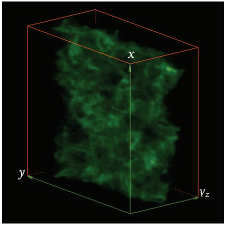

Observational diagnostics

- High-resolution spectroscopy

  ☞ $\delta\vec{v}$

- High-resolution imaging (CO, HI, Hα, dust ...)

  ☞ δn

Map of Draco nebula

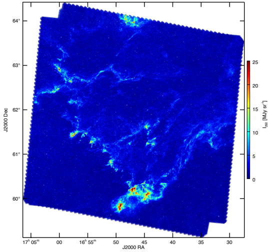

$\Rightarrow$

Density histogram

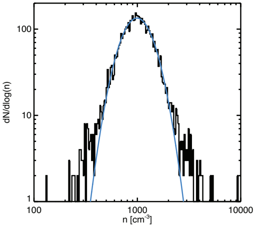

Herschel-SPIRE 250 μm *(Miville-Deschênes et al. 2017)*

Observational diagnostics

- High-resolution spectroscopy

  ☞ $\delta\vec{v}$

- High-resolution imaging (CO, HI, Hα, dust ...)

  ☞ δn

- Polarization observations
  (synchrotron, dust, stars ...)

  ☞ $\delta\vec{B}$

Dust polarized emission

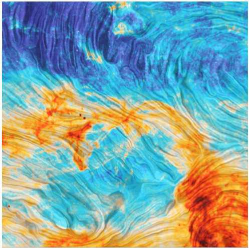

Planck Collaboration (2015)

Observational diagnostics

- High-resolution spectroscopy

  ☞ $\delta\vec{v}$

- High-resolution imaging (CO, HI, Hα, dust ...)

  ☞ δn

- Polarization observations (synchrotron, dust, stars ...)

  ☞ $\delta\vec{B}$

- Effects of radio wave propagation

  ☞ δn_{e} , δB in warm ionized medium [WIM]

Outline

1. Introduction
2. Effects of radio wave propagation
   - Dispersion of pulsar signals
   - Interstellar scattering
   - Faraday rotation
3. Radio polarized emission
   - Synchrotron emission
   - Faraday tomography

Radio wave propagation || $\vec{B}_0$

- Dispersion relation

$$\omega^2 = c^2\,k^2 + \frac{\omega_e^2}{1 \pm \frac{\Omega_e}{\omega}}$$

with $\omega_e = \sqrt{\frac{4\pi\, n_e\, e^2}{m_e}}$ (plasma frequency)

$\Omega_e = \frac{-e\,B}{m_e\,c}$ (electron gyro-frequency)

In WIM: $|\Omega_e| \ll \omega_e \lll \omega$

- Refractive index

$$n^2 \equiv \frac{c^2\,k^2}{\omega^2} = 1 - \frac{\frac{\omega_e^2}{\omega^2}}{1 \pm \frac{\Omega_e}{\omega}}$$

- Plasma effects
  - 1^{st} order correction $\propto \omega_e^2 \propto n_e$
  - 2^{nd} order correction $\propto \Omega_e \propto B$

Outline

Governing equations

To 1^{st} order in $\frac{\omega_e}{\omega}$, $\frac{\Omega_e}{\omega}$

- Dispersion relation

$$\omega^2 = c^2 k^2 + \omega_e^2 = c^2 k^2 + \frac{4\pi n_e e^2}{m_e}$$

- Group velocity

$$V_g = \frac{\partial \omega}{\partial k} = c \left(1 - \frac{\omega_e^2}{2\,\omega^2}\right) = c \left(1 - \frac{e^2}{2\pi\, m_e\, c^2}\, n_e\, \lambda^2\right)$$

- Travel time

$$t_{tr} = \int_{src}^{obs} \frac{ds}{V_g} = \frac{L}{c} + \frac{e^2}{2\pi\, m_e\, c^3} \underbrace{\left(\int_{src}^{obs} n_e\, ds\right)}_{\mathrm{DM}} \lambda^2$$

Census of Galactic pulsars

- Currently known
  - Total number : 2 702
  - With measured DMs : 2 607
  - With measured RMs : 1 159

(ATNF pulsar catalogue, version 1.60, *Manchester et al. 2005*$^{+}$)

- Expected with SKA 1
  - Total number : ~ 18 000
  - Most with measured DMs & RMs
  - Density in Galactic plane : ~ 6 deg^{-2}

(*Keane et al. 2015*)

Pulsars with known distances

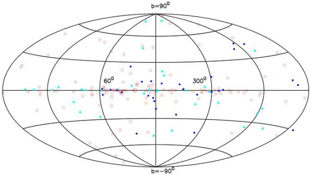

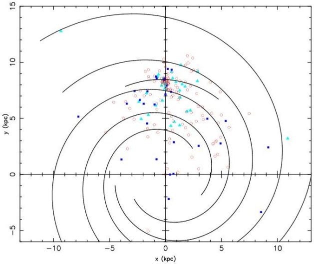

Yao, Manchester, & Wang (2016)

Outline

Physical picture

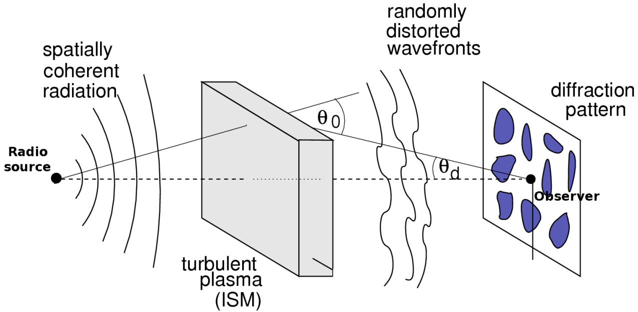

Figure credit: *Lorimer & Kramer* (Handbook of Pulsar Astronomy)

Governing equations

In the presence of interstellar fluctuations

- **Refractive index**

$$\mathrm{n}^2 \;=\; 1 - \frac{\omega_e^2}{\omega^2} \;=\; 1 - \frac{4\pi\, n_e\, e^2}{m_e\, \omega^2}$$

- **Phase fluctuation**

$$\delta\phi \;=\; \int_{\mathrm{src}}^{\mathrm{obs}} \delta\mathrm{n}\;\, k\, ds \;=\; \underbrace{\frac{e^2}{m_e\, c^2}}_{r_e}\; \lambda \left(\int_{\mathrm{src}}^{\mathrm{obs}} \delta n_e\; ds\right)$$

- **Phase structure function**

$$\mathcal{S}_\phi\,(\vec{r_1} - \vec{r_2}) \;=\; \left\langle \left[\, \delta\phi(\vec{r}_1) \;-\; \delta\phi(\vec{r_2})\,\right]^2 \right\rangle$$

- **Visibility function** (measured by interferometer)

$$V(\vec{r}) \;=\; \exp\left(-\,\tfrac{1}{2}\,\mathcal{S}_\phi(\vec{r})\right)$$

Phase structure function

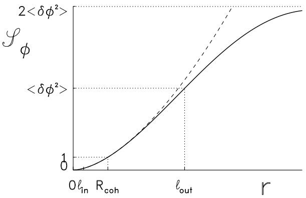

Visibility function

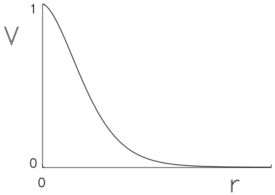

Phase structure function $\rightarrow$ power spectrum of δn_e

- In general

$$\langle \delta n_e^2 \rangle = \int P_n(\vec{q})\, d\vec{q}$$

- For isotropic turbulence

$$\langle \delta n_e^2 \rangle = \int P_n(q)\, 4\pi\, q^2\, dq = \int E_n(q)\, dq$$

$$\Rightarrow \quad S_\phi(r) = r_e^2\, \lambda^2 \int_{\rm src}^{\rm obs} \left(\int {\rm fc}(qr)\, \frac{E_n(q)}{q}\, dq \right) ds$$

dominated by $\boxed{q\,r \sim 1}$

- If power-law spectrum

$$E_n(q) = 4\pi\, C_n^2\, q^{-\alpha}$$

(with $0 < \alpha < 2$)

$$\Rightarrow \quad S_\phi(r) = {\rm fc}(\alpha)\, r_e^2\, \lambda^2 \underbrace{\left(\int_{\rm src}^{\rm obs} C_n^2\, ds \right)}_{\rm SM} r^\alpha$$

Phase structure function $\longrightarrow$ power spectrum of δn_e

What have we learned ?

- Power law index

$\alpha \simeq \frac{5}{3} \quad \Rightarrow$ Kolmogorov turbulence

- Inner scale

$\ell_{in} \sim \begin{cases} (50 - 200) \text{ km} \\ 300 \text{ km} \end{cases}$ (*Spangler & Gwinn 1990*) (*Molnar et al. 1995*) ☞

$\Rightarrow \quad \ell_{in} \sim \begin{cases} \frac{V_A}{\Omega_i} & \text{(proton inertial length)} \\ r_{g,i} & \text{(proton gyro-radius)} \end{cases}$

⚠ Only for LOS toward H II regions

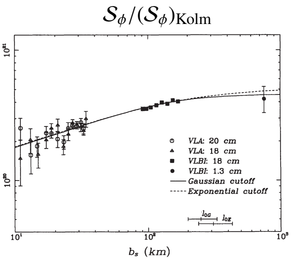

Interstellar scintillations

Interstellar scintillations (ISS) = intensity fluctuations

- Weak ISS $\left(\delta I_{\rm rms} \ll \langle I \rangle\right)$

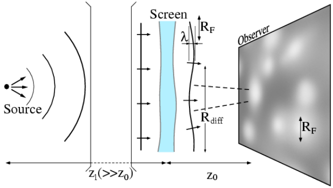

Figure Credit: *M. Moniez*

- Diffractive

$$R_{\rm weak} \approx R_{\rm F} \equiv \sqrt{\frac{L}{k}}$$
$$\sim 10^6 \text{ km}$$

Interstellar scintillations

Interstellar scintillations (ISS) = intensity fluctuations

- Strong ISS $\left(\delta I_{\rm rms} \simeq \langle I \rangle\right)$

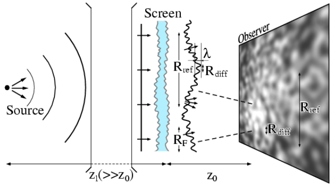

Figure Credit: *M. Moniez*

- Diffractive

$$R_{\rm diff} \approx R_{\rm coh} \quad \rightsquigarrow \quad S_\phi(R_{\rm coh}) = 1$$
$$\sim (10^3 - 10^5)\ {\rm km}$$

- Refractive

$$R_{\rm ref} \approx R_{\rm sc} \equiv \frac{L}{k\,R_{\rm coh}}$$
$$\sim (10^7 - 10^9)\ {\rm km}$$

Other effects of interstellar scattering

- Angular broadening of point sources

  For strong ISS : $\Delta\theta = \dfrac{1}{k\,R_{\rm coh}}$

- Angular wandering

- Temporal broadening of pulsar pulses

  For strong ISS : $\Delta t \propto \dfrac{L\,\Delta\theta^2}{c}$

- Fluctuations in pulse arrival times

- Time & frequency modulations in pulsar dynamic spectra
  - Drifting bands
  - Criss-cross patterns, periodic patterns
  - Changes in frequency decorrelat° bandwidth

Pulsar dynamic spectrum

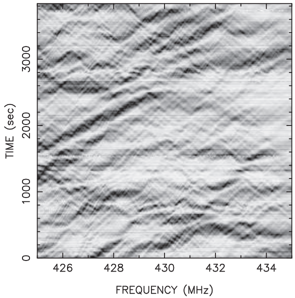

Lazio et al. (2004)

Complete power spectrum of δn_e

- Compilation of interstellar scattering data

  ☞ Single power law : $E_n \propto q^{-\frac{5}{3}}$ (Kolmogorov)

  for $\ell \approx (10^3\ \mathrm{km} - 10^{10}\ \mathrm{km})$

  ↳ 100 AU

Big power-law in the sky

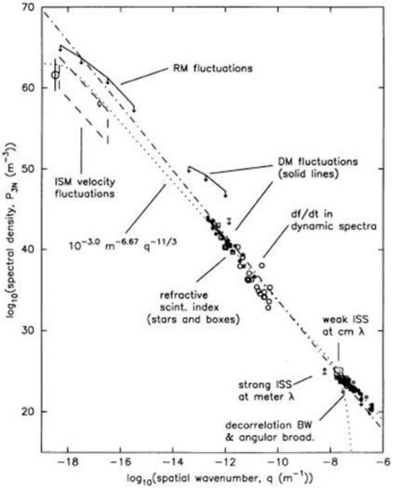

Armstrong, Rickett, & Spangler (1995)

Complete power spectrum of δn_e

- Compilation of interstellar scattering data

  ☞ Single power law : $E_n \propto q^{-\frac{5}{3}}$ (Kolmogorov)

  for $\ell \approx (10^3 \text{ km} - 10^{10} \text{ km})$

  ↳ 100 AU

- Combined with data at large scales

  ☞ Single power law : $E_n \propto q^{-\frac{5}{3}}$ (Kolmogorov)

  for $\ell \approx (10^3 \text{ km} - 10^{15} \text{ km})$

  ↳ 30 pc

Big power-law in the sky

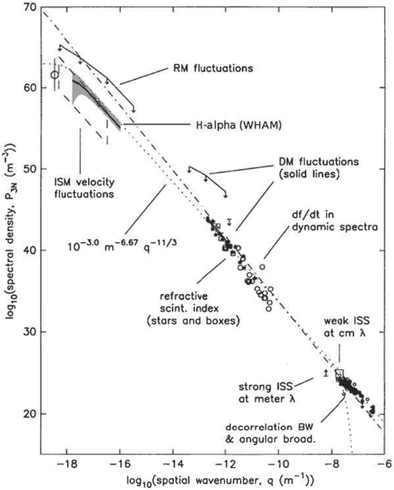

Chepurnov & Lazarian (2010)

Anisotropy of turbulence

Elongated images of strongly scattered extragalactic sources

Visibility function along major & minor axes

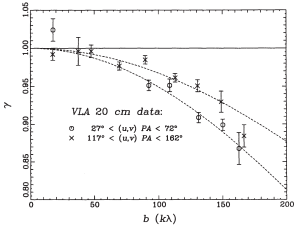

Molnar et al. (1995)

- ☞ Anisotropic density fluctuations
- ☞ Evidence for interstellar magnetic field

Outline

Governing equations

To 2^{nd} order in $\dfrac{\omega_e}{\omega}, \dfrac{\Omega_e}{\omega}$

- **Dispersion relation**

$$\omega^2 = c^2 k^2 + \omega_e^2 \mp \frac{\omega_e^2 \, \Omega_e}{\omega}$$

with $\omega_e = \sqrt{\dfrac{4\pi \, n_e \, e^2}{m_e}}, \quad \Omega_e = \dfrac{-e \, B}{m_e \, c}$

- **Phase velocity**

$$V_\phi = \frac{\omega}{k} = c \left(1 + \frac{\omega_e^2}{2\,\omega^2} \mp \frac{\omega_e^2 \, \Omega_e}{2\,\omega^3} \right)$$

- **Phase difference between R-mode & L-mode**

$$\Delta\phi = \int_{\text{src}}^{\text{obs}} \frac{\Delta V_\phi}{c} \, k \, ds = \int_{\text{src}}^{\text{obs}} \frac{\omega_e^2 \, |\Omega_e|}{\omega^3} \, k \, ds$$

- **Rotation of polarization angle**

$$\Delta\psi = \frac{1}{2} \Delta\phi = \underbrace{\frac{e^3}{2\pi \, m_e^2 \, c^4} \left(\int_{\text{src}}^{\text{obs}} n_e \, B \, ds \right)}_{\text{RM}} \lambda^2$$

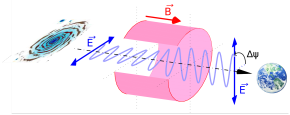

Figure Credit: *Philippe Terral*

Physical picture

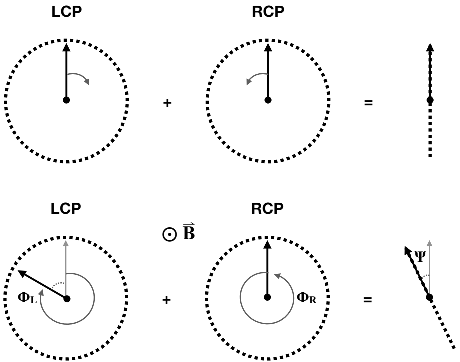

Figure credit: *Jennifer West*

Power spectra from extragalactic RMs

Combine measured $\mathrm{RM} = C \int n_\mathrm{e} \, B_\parallel \, ds$ & $\mathrm{EM} = \int n_\mathrm{e}^2 \, ds$

to derive power spectra of δn_e and δB separately

(Minter & Spangler 1996)

Structure function of RM

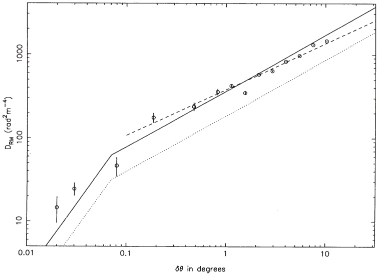

Structure function of EM

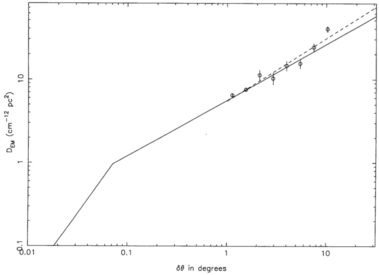

☞ $$\mathcal{S}_\mathrm{RM},\ \mathcal{S}_\mathrm{EM} \propto \begin{cases} \delta\theta^{\frac{5}{3}} & \text{for} \quad \delta\theta < 0.07^\circ \\ \delta\theta^{\frac{2}{3}} & \text{for} \quad \delta\theta > 0.07^\circ \end{cases}$$

Power spectra from extragalactic RMs

Combine measured $\mathrm{RM} = C \int n_e \, B_\parallel \, ds$ & $\mathrm{EM} = \int n_e^2 \, ds$

to derive power spectra of δn_e and δB separately *(Minter & Spangler 1996)*

☞ $$S_{\mathrm{RM}}, S_{\mathrm{EM}} \propto \begin{cases} \delta\theta^{\frac{5}{3}} & \text{for} \quad \delta\theta < 0.07^\circ \\ \delta\theta^{\frac{2}{3}} & \text{for} \quad \delta\theta > 0.07^\circ \end{cases}$$

$$\Rightarrow \quad E_n, E_B \propto \begin{cases} q^{-\frac{5}{3}} & \text{for} \quad \ell < 3.6 \text{ pc} \\ q^{-\frac{2}{3}} & \text{for} \quad 3.6 \text{ pc} < \ell \lesssim 100 \text{ pc} \end{cases}$$

(assuming $L = 2.9$ kpc)

$$\delta B_{\mathrm{rms}} \sim 1 \ \mu\mathrm{G} \qquad \text{for} \quad \ell < 3.6 \text{ pc}$$

☞ - True MHD turbulence
- 3D Kolmogorov for $\ell \lesssim 4$ pc & 2D for $\ell \approx (4 - 100)$ pc
- Possibly turbulent sheets / filaments of thickness ~ 4 pc

Outer scale from extragalactic RMs

Structure function of RM

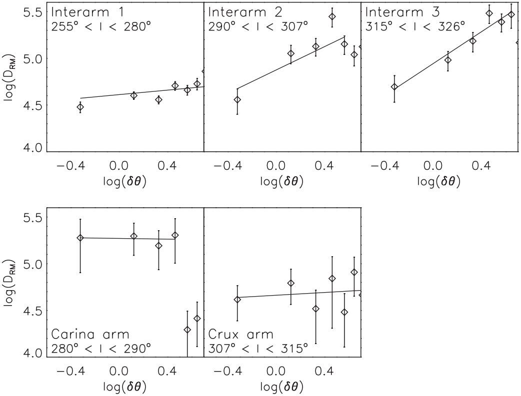

Haverkorn et al. (2008)

- In interarm regions
  - Kolmogorov for $\ell \lesssim$ a few pc
  - Flatter for $\ell \approx$ (a few – 100) pc
  - $\Rightarrow \ell_{\rm out} \sim 100$ pc
- In spiral arms
  - Kolmogorov for $\ell \lesssim$ a few pc
  - Flat for $\ell \gtrsim$ a few pc
  - $\Rightarrow \ell_{\rm out} \sim$ a few pc

Power spectrum from Galactic pulsar RMs

Combine measured $\mathrm{RM} = C \int_0^L n_e \, B_\parallel \, ds$ & $\mathrm{DM} = \int_0^L n_e \, ds$ & L

to derive power spectrum of δB at large scales

(Han et al. 2004)

Magnetic energy spectrum

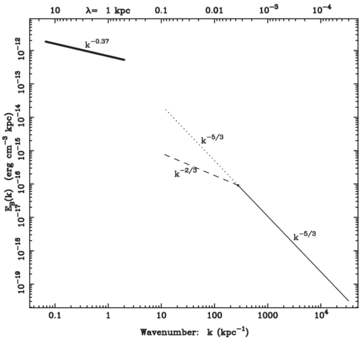

☞ $E_B \propto q^{-0.37}$

for $\ell \approx (0.5 - 15)$ kpc

$\delta B_{\mathrm{rms}} \sim 6 \, \mu\mathrm{G}$

Prospects for RM grids

- Pulsars with measured DMs & RMs

  * Currently : 1 159

    (ATNF pulsar catalogue, version 1.60, *Manchester et al. 2005*$^{+}$)

  * Expected with SKA 1 :

    - Total number : $\sim$ 18 000
    - Density in Galactic plane : $\sim$ 6 deg^{-2}

    (*Keane et al. 2015*)

- Extragalactic sources with measured RMs

  * Currently : $\simeq$ 45 000

    (*Oppermann et al. 2015* + *Schnitzeler et al. 2019*)

  * Expected with SKA 1 :

    - Total number : $\sim (1-4)\times 10^{7}$
    - Average density : $\sim$ (300 - 1 000) deg^{-2}

    (*Haverkorn et al. 2015*)

Outline

Outline

Total & polarized intensities

$\mathcal{E} = f(\alpha)\, n_{\rm CRe}\, B_\perp^{\,\alpha+1}\, \nu^{-\alpha}$ & $\vec{\mathcal{E}}_{\rm pol} \perp \vec{B}_\perp$

- Total intensity : $I = \int \mathcal{E}\, ds$ ☞ $B_\perp$ (strength only)
- Polarized intensity : $\vec{P} = \int \vec{\mathcal{E}}_{\rm pol}\, ds$ ☞ $(\vec{B}_{\rm ord})_\perp$ (strength & orientation)

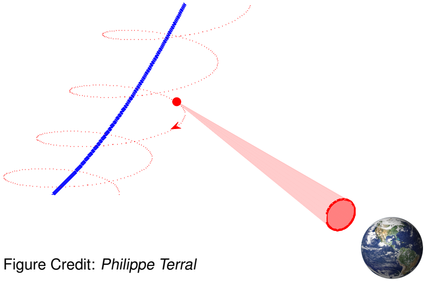

Figure Credit: *Philippe Terral*

Total & polarized intensities

$\mathcal{E} = f(\alpha)\, n_{\rm CRe}\, B_\perp^{\alpha+1}\, \nu^{-\alpha}$ & $\vec{\mathcal{E}}_{\rm pol} \perp \vec{B}_\perp$

- Total intensity : $I = \int \mathcal{E}\, ds$ ☞ $B_\perp$ (strength only)

- Polarized intensity : $\vec{P} = \int \vec{\mathcal{E}}_{\rm pol}\, ds$ ☞ $(\vec{B}_{\rm ord})_\perp$ (strength & orientation)

↳ $Q + i\,U = \int \mathcal{E}_{\rm pol}\, e^{2i\psi}\, ds$

Total & polarized intensities

$\mathcal{E} = f(\alpha)\, n_{\rm CRe}\, B_\perp^{\;\alpha+1}\, \nu^{-\alpha}$ & $\vec{\mathcal{E}}_{\rm pol} \perp \vec{B}_\perp$

- Total intensity : $I = \int \mathcal{E}\, ds$ ☞ $B_\perp$ (strength only)

- Polarized intensity : $\vec{P} = \int \vec{\mathcal{E}}_{\rm pol}\, ds$ ☞ $(\vec{B}_{\rm ord})_\perp$ (strength & orientation)

☞ $B \sim 5\ \mu$G

$B_{\rm ord} \sim 3\ \mu$G

$\Rightarrow \delta B_{\rm rms} \sim 5\ \mu$G

Fluctuations in *total* intensity

Theoretical developments *(Lazarian & Pogosyan 2012)*
& numerical simulations *(Herron et al. 2016)*

☞ Synchrotron intensity fluctuations are anisotropic, forming filaments $\parallel \vec{B}_{\perp}$

Synchrotron total intensity map

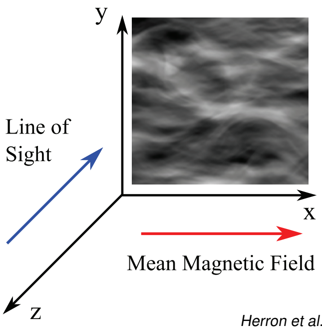

Herron et al. (2016)

Fluctuations in *total* intensity

Synchrotron intensity gradients ☞ orientation of $\vec{B}_\perp$

Synchrotron intensity gradients & polarization vectors (Planck)

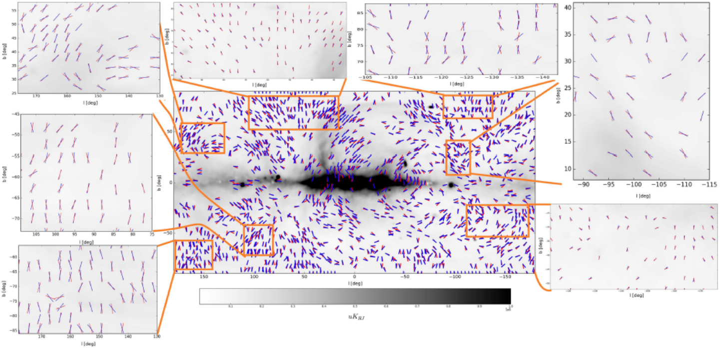

Lazarian et al. (2017)

Synchrotron power spectrum

Angular power spectrum of synchrotron TI

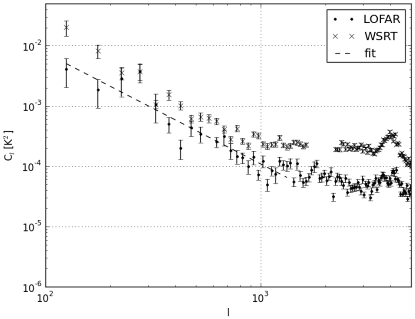

Iacobelli et al. (2013)

☞ $C_l \propto l^{-1.84}$

for $l \approx (100 - 1\,300)$

$\delta\theta \approx (8' - 110')$

$\Rightarrow \ell_{\rm out} \lesssim 20$ pc

$\Rightarrow \dfrac{B_{\rm ord}}{\delta B_{\rm rms}} \lesssim 0.3$

Fluctuations in *polarized* intensity

Total & polarized intensities at 1.4 GHz (ATCA)

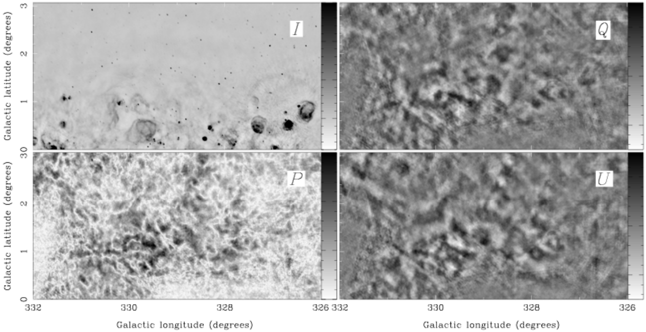

Gaensler et al. (2011)

☞ Filamentary structures in P, with no counterparts in I

- Arise from fluctuations in Faraday rotation
- Probe magneto-ionic turbulence in WIM

Fluctuations in *polarized* intensity

Measure synchrotron polarization gradients

$|\nabla\vec{P}|$ at 1.4 GHz (ATCA)

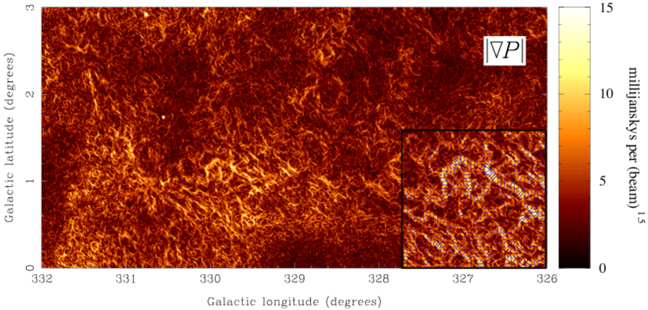

Gaensler et al. (2011)

Compare with 3D MHD simulations

☞ Turbulence in WIM is subsonic or trans-sonic ($\mathcal{M}_s \lesssim 2$) *(Burkhart et al. 2012)*

Fluctuations in *polarized* intensity

- Synchrotron polarization gradients ☞ orientation of $\vec{B}_\perp$
  Measurements at several λ ☞ Info on LOS distribution

Synchrotron polarizat° gradients & polarizat° vectors (from simulat°)

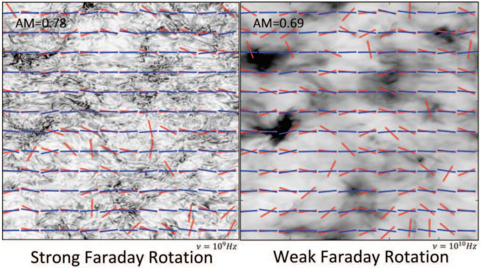

Lazarian & Yuen (2018)

- Gradients of $\dfrac{dP}{d\lambda^2}$ ☞ $B_\parallel$

Outline

General concept

- Underlying processes

  - Galactic synchrotron emission : linearly polarized

  - Faraday rotation : λ-dependent

- General idea

  - Measure synchrotron polarized intensity at many different λ

  - Convert λ-dependence into s-dependence

- Output

  Faraday cube = 3D cube of synchrotron polarized emission as fc(α, δ, Φ)

General method

- Faraday rotation of background source

$$\Delta\psi = \mathrm{RM}\ \lambda^2 \quad \text{with} \quad \mathrm{RM} = C \int_0^L n_e\, B_{\|}\, ds \quad \text{(rotation measure)}$$

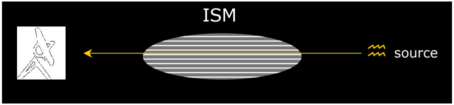

- Faraday rotation of Galactic synchrotron emission

Synchrotron emission & Faraday rotation are *spatially mixed*

$$\vec{P}(\lambda^2) = \int \vec{F}(\Phi)\, e^{2i\Phi\lambda^2}\, d\Phi \quad \text{with} \quad \Phi(z) = C \int_0^z n_e\, B_{\|}\, ds \quad \text{(Faraday depth)}$$

Fourier transform $\Rightarrow$ $\vec{F}(\Phi) = \frac{1}{\pi} \int \vec{P}(\lambda^2)\, e^{-2i\Phi\lambda^2}\, d\lambda^2$

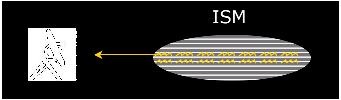

Figure Credit: *Marijke Haverkorn*

Faraday spectrum

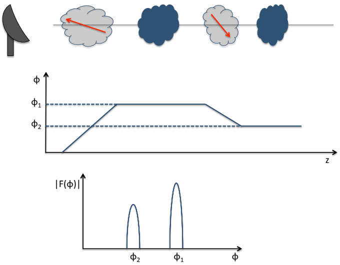

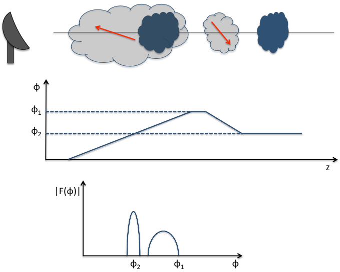

Figure Credit: *Marta Alves*

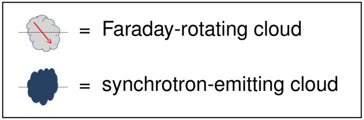

Faraday cube

For given sky area

- Derive Faraday spectrum, $\vec{F}(\Phi)$, in many directions (α, δ)
- Combine all derived Faraday spectra into Faraday cube = 3D cube of $\vec{F}(\alpha, \delta, \Phi)$

Faraday cube toward Fan region, obtained with LOFAR *(van Eck et al. 2017)*

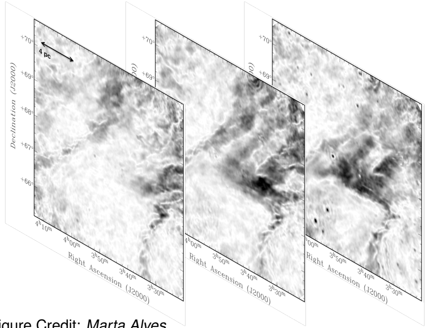

Figure Credit: *Marta Alves*

3 slices at

$$\Phi_1 = -2.0 \text{ rad m}^{-2}$$
$$\Phi_2 = -1.5 \text{ rad m}^{-2}$$
$$\Phi_3 = -1.0 \text{ rad m}^{-2}$$

Expected results

- From synchrotron polarized intensity map to Faraday cube
  - Measure $\vec{P}(\lambda^2)$ at many different λ
  - Fourier transform $\vec{P}(\lambda^2)$ to obtain $\vec{F}(\Phi)$
- From Faraday cube to physical space
  - Uncover synchrotron-emitting & Faraday-rotating features in Faraday cube
  - Identify these features with interstellar matter structures
- For synchrotron-emitting regions

  $\int \vec{F}(\Phi)\, d\Phi$ ☞ $\vec{B}_\perp$
- For Faraday-rotating regions

  $\Delta\Phi$ ☞ $B_\parallel$

To conclude

- Effects of radio wave propagation
  - ☞ Best method to probe δn_e at small scales
- Radio polarized emission
  - ☞ Information on δB